



Metabolite analysis in the type 1 diabetic mouse model

Sung Jean Park*

College of Pharmacy and Gachon Institute of Pharmaceutical Sciences, Gachon University, 191 Hambakmo-ero, Yeonsu-gu, Incheon 21936, Republic of Korea

Received September 2, 2021; Revised September 14, 2021; Accepted September 14, 2021

Abstract Type 1 diabetes mellitus (T1DM) is caused by insufficient production of insulin, which is involved in carbohydrate metabolism. Type 2 diabetes mellitus (T2DM) has insulin resistance in which cells do not respond adequately to insulin. The purpose of this study was to estimate the characteristics of type 1 diabetes using streptozotocin-treated mice (STZ-mouse). The sera samples were collected from the models of hyperglycemic mouse and healthy mouse. Based on the pair-wise comparison, five metabolites were found to be noticeable: glucose, malonic acid, 3-hydroxybutyrate, methanol, and tryptophan. It was very natural glucose was upregulated in STZ-mouse. 3-hydroxybutyrate was also increased in the model. However, malonic acid, tryptophan, and methanol was downregulated in STZ-mouse. Several metabolites acetoacetate, acetone, alanine, arginine, asparagine, histidine, lysine, malate, methionine, ornithine, proline, propylene glycol, threonine, tyrosine, and urea tended to be varied in STZ-mouse while the statistical significance was not stratified for the variation. The multivariate model of PCA clearly showed the group separation between healthy control and STZ-mouse. The most significant metabolites that contributed the group separation included glucose, citrate, ascorbate, and lactate. Lactate did not show the statistical significance of change in t-test while it tends to down-regulated both in DNP and Diabetes.

Keywords Diabetes, Type I, Metabolite, NMR, Streptozotocin

Introduction

Diabetes mellitus is a disease in which blood glucose levels rise due to decreased insulin secretion from pancreatic β -cells or insulin resistance in peripheral tissues due to genetic, metabolic, and environmental factors.^{1,2} The onset of diabetes is strongly related to free radicals. It is known that the production of free radicals is increased by many biochemical pathways such as glucose autooxidation, polyol pathway, protein glycosylation, etc.³⁻⁵ In addition, in diabetes, oxidative stress and oxidative damage to tissues may be increased by several factors. This oxidative stress is believed to be related to eating habits and lifestyle habits such as drinking and smoking.⁶ Recently, many investigation have been reported on the prevention of oxidative stress and improvement of the antioxidant defense system in the body through a natural diet for the prevention or treatment of diabetes.⁷ Natural materials including non-flavonoid polyphenols such as resveratrol and curcumin, flavonoids such as epigallocatechin and quercetin, vegetables and other products such as green tea, and rowanberry may be a dietary alternatives for pharmacological therapy.⁸ Diabetic complications are caused by simultaneous damage to microvessels and large blood vessels in the

* Address correspondence to: **Sung Jean Park**, College of Pharmacy and Gachon Institute of Pharmaceutical Sciences, Gachon University, 191 Hambakmo-ero, Yeonsu-gu, Incheon 21936, Republic of Korea. Tel: 82-32-820-4957; E-mail: psjnmr@gachon.ac.kr

body due to continuous high blood sugar, which can lead to end-stage renal failure, amputation of an uninjured limb due to delayed wound healing, and blindness due to retinopathy.^{9,10} Diabetic peripheral neuropathy is one of the complications of diabetes, and it is a disease that causes various problems due to nerve damage caused by diabetes for a long time. It can appear in any nervous system, but it is most common in the peripheral nervous system. That is, nerve fibers are damaged directly from high glucose level, resulting in diabetic peripheral neuropathy (DN). Previously we showed the metabolomic characteristic of DN and Diabetes investigated with NMR spectroscopy.¹¹ Multiple combinations of lactate and citrate in the OPLS-DA model we proposed resulted in good discrimination between DN patients and healthy control, with ROC value of 0.952.

Since diabetes is characterized by high sugar levels, it is of course closely related to the energy metabolism of cells. It is natural that the broken energy metabolism leads to abnormalities in insulin.¹² Insulin is also present in the brain and brain cell death was observed when brain insulin levels are low.¹³ In addition, it has also been reported to play an important role in learning and memory formation.¹⁴ Therefore, it would be meaningful to study the correlation between brain energy metabolism, insulin, and diabetes.¹⁵

In this study, we aimed to identify metabolic characteristic of streptozotocin-derived diabetic mouse model by the NMR-based study. We monitored the quantitative alteration of serum metabolites in both healthy and disease mice and compared the several metabolites with the healthy controls. The statistical analysis of NMR metabolites showed some fluctuation of metabolites probable model of discrimination of disease.

Experimental Methods

Animals- Male C57BL/6 mice were purchased from Orient Bio (Seongnam-Si, Korea). The animal experiments were carried out following Institutional Animal Care and Use guidelines of Lee Gil Ya Cancer

and Diabetes Institute (LCDI) at Gachon University. Mice were housed in groups of 3–5 animals/cage under a controlled environment with a light cycle of 12 h/12 h of day/night, temperature of 22 ± 2 °C, and a relative humidity of $60 \pm 10\%$. Mice had free access to food and water. Mice with similar physical characteristics (i.e., similar age and body weight) were randomly divided ($n = 5$) into two groups: Con, vehicle-treated non-diabetic control group; STZ, vehicle and STZ-treated group. Type 1 diabetes was induced by intraperitoneal (i.p.) injection of 50 mg/kg/day STZ (Sigma, St Louis, MO, USA) freshly prepared in 0.1 M sodium citrate buffer, pH 4.5, for 5 consecutive days. Mice with blood glucose levels above 300 mg/dL were considered diabetic.

NMR sample preparation - Blood samples (100 μ l) were collected and all blood was drawn by the same operator. Whole blood was centrifuged at $12,000 \times g$ for 10 minutes and supernatant was removed. Serum was collected in serum-separator tubes and stored at -80°C until NMR test. The 100 μ l serum aliquots of healthy controls and STZ-mouse were mixed with the 400 μ l stock solution of NMR buffer containing 550 mM sodium phosphate buffer. The final NMR samples contained 100 mM sodium phosphate buffer (pH 7.0), 2 mM of trimethylsilyl-propanoic acid (TSP) and 10 % D_2O . To analyze the metabolites, 1D Carr-Purcell-Meiboom-Gill (CPMG) NMR spectra (cpmgrp1d) were obtained at 298 K on a Bruker ASCENDIII 600 spectrometer equipped with a cryoprobe.¹⁶ The CPMG pulse sequence generated spectra edited by T2 relaxation times, reducing broad resonances from high molecular weight compounds, improving the observation of low molecular weight metabolites. The water signal was removed by a presaturation method using low-power irradiation on the water resonance. ^1H NMR spectrum for each sample consisted of 128 scans with following parameters: spectral width = 12019.2 Hz, spectral size = 65,536 points, pulse width (90) = 13.2 μ s and relaxation delay (RD) = 2.0 s. Each free induction decay (FID) was zero-filled to 64,000 points and transformed with line broadening (LB) = 0.3 Hz. Data were processed using NMRPipe and analyzed using Mnova.

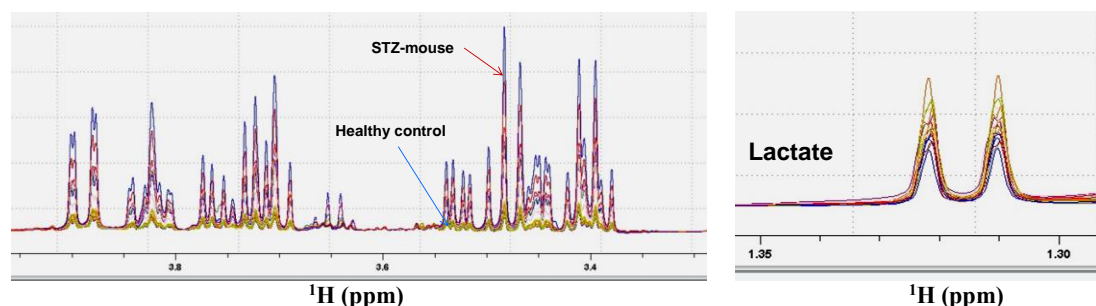


Figure 1. Overlay of NMR spectra obtained from STZ-mouse and healthy control. The glucose region (left panel) and lactate region (right panel) are presented, respectively. The STZ-mouse showed high intensity of glucose peaks (blue and red colors) and the healthy control showed low intensity of glucose peaks (yellow color).

NMR processing and assignment - Initially, ^1H NMR spectra were manually phased and baseline corrected using Bruker Topspin 3.2 software (Bruker GmbH, Karlsruhe, Germany) and referenced to TSP at 0.0 ppm. The post-processing baseline correction was conducted with Mnova (Mestrelab Research, Santiago, Spain). In each spectrum, the algorithm of multipoint baseline correction was used for building the baseline model. Because the NMR spectral bins of each spectrum can be easily influenced by small change of pH and/or ionic strength and the broad bin size consisting of more than one resonance often makes the result difficult to interpret, the peak alignment using segment and pair-wise peak alignment by Mnova was applied before binning. In addition, a variable bin size ranging from 0.005 ppm to 0.09 ppm was used so that each single bin contains single metabolic information as much as possible. The ^1H NMR spectra were segmented into variable-sized spectral regions (bins) between 0.94 and 8.48 ppm. The chemical shift region of 4.69–5.2 ppm containing residual water was excluded. The lipid or protein contaminated region (1.10–1.33, 1.52–1.68, 1.78–1.90, and 5.28–5.70 ppm) was also removed from the spectra to clarify the contribution of metabolites.¹⁷ The integrated bins were used as the variables for statistics. The assignment of bins was achieved using Chenomx NMR suite 7.7 (Chenomx Inc., Edmonton, Canada) and evaluated in ^1H - ^{13}C HSQC and 2D ^1H - ^1H TOCSY spectra.

Statistical analysis - The statistical analysis was

carried out using the SIMCA 15 (Umetrics, Umea, Sweden),¹⁸ and SPSS 23 (SPSS, Inc., an IBM Company, Chicago, Illinois, USA). The spectra were classified into controls and clinically diagnosed case subjects (diabetic neuropathy and diabetes). The integrated bins were normalized using probabilistic quotient normalization (PQN) algorithm to facilitate comparison of samples. In order to provide a reasonable balance of contributions from high and low amplitude signals, the spectral integrals (bins) were scaled by the procedure called pareto-scaling: each variable is mean-centered and divided by the square root of the standard deviation.^{19, 20}

The multivariate analysis was performed as follows. To clarify the separation between groups, bin data were processed using an unsupervised pattern recognition method, principal component analysis (PCA).^{21, 22} The loading-plot is an easy method to visualize significant features (variables) of an PCA model of two classes. The metabolites affected with the group separations were identified by the corresponding loading-plot, in which each point represented a single bin data. The efficiency and reliability of PCA models was validated using 500-random permutation test.²³ Corresponding Mahalanobis p-values for PCA score plots were calculated with PCA/PLS-DA utilities to determine the statistical significance of group separation in the PCA score plots.²⁴ An observed p-value of 0.05 was used to identify statistically significant group separation. Univariate analysis was also performed to

Table 1. Statistical analysis using the non-parametric Kruskal-Wallis test

Assigned metabolite	Adjusted <i>p</i> -value *	FDR ***	Metabolic change ****
Glucose	<0.001	<0.05	△
3-Hydroxybutyrate	<0.01	<0.05	△
Malonate	<0.01	<0.05	▽
Tryptophan	<0.01	<0.05	▽
Methanol	<0.01	<0.05	▽

* Adjusted *p*-value was calculated by Bonferroni's correction.

** HC, healthy control; STZ, STZ-mouse

*** FDR was calculated by Benjamini-Hochberg method.

**** Compared to the values of healthy controls, △ indicates increase and ▽ indicates decrease.

identify how significantly each bin affects the difference between groups. The Kruskal-wallis test (non-parametric analysis) was used for the comparative analysis.²⁵

Results and Discussion

NMR spectra of STZ-mouse - Serum samples from 5 healthy controls (HC) and 5 STZ-mice were obtained. The CPMG spectrum of each sample was measured around 1 hr. The figure 1 shows the overlay of all spectra. The glucose region and lactate region were selected to be shown.

Univariate analysis- The statistical capability of the metabolites to differentiate between groups, means of metabolite bins were compared. Table 1 shows the

result of univariate analysis, that is, the non-parametric Kruskal-Wallis test among healthy control, and STZ-mouse. The bin table created for the multivariate analysis was used as input variable for calculating *p*-value and adjusted *p*-value was calculated by Bonferroni's correction.²⁶ Null hypotheses of no difference were rejected if the adjusted *p*-values by Benjamini and Hochberg FDR were less than 0.05. As a result, five metabolites listed in the Table 1 showed significant difference between groups. Two metabolites of glucose and 3-hydroxybutyrate were higher in the STZ-mouse compared to the HC group. The malonate, tryptophan, and methanol were significantly reduced in the STZ-mouse. In addition, several metabolites acetoacetate, acetone, alanine, arginine, asparagine, histidine, lysine, malate, methionine, ornithine, proline, propylene glycol, threonine, tyrosine, and urea tended

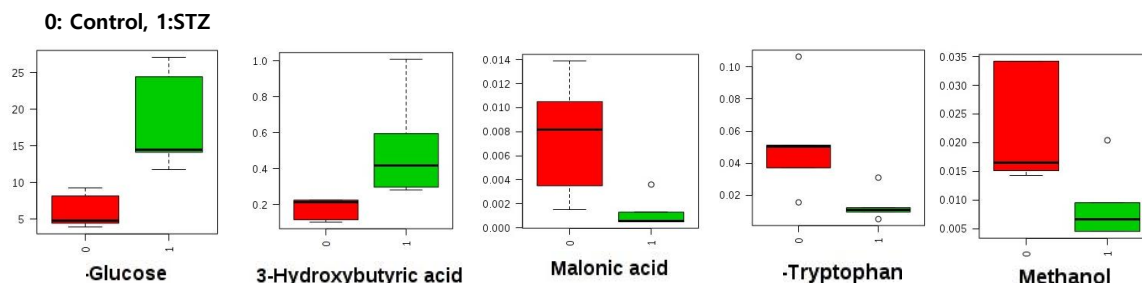


Figure 2. Box and Whisker plots of representative metabolites. The horizontal line in the middle portion of the box is median value. The bottom and top boundaries of boxes represent lower and upper quartile. The open circles represent outliers.

to be varied in STZ-mouse even though the statistical significance was not stratified for the variation (data not shown). Box and whisker plots of five statistical significant metabolites, contributing to group separation, were illustrated in the figure 2.

PCA was used as a unsupervised statistical method to clarify the separation between two groups. The 2D score plot of PCA for healthy control and STZ-mouse is shown in the figure 3. Consistent with univariate analysis, PCA plot showed clear separation. The contribution of metabolites such as glucose, 3-hydroxybutyrate, malonate, and tryptophan to separation of group is well recognized on the loading plot. Both the univariate and multivariate analysis suggests that the variation of five metabolites is very important in the metabolism of the type I diabetic model.

Conclusion

Through this study, we found that five metabolites were particularly significantly altered in the streptozotocin-induced diabetes model. The change in glucose is natural, but the significant change in the remaining 4 metabolites is a very interesting phenomenon. An increase in 3-hydroxybutyrate, one of the blood ketones, is very likely a result of ketoacidosis caused by diabetes. Although the decrease in malonate related to fatty acid metabolism was unexpected, the report that methylmalonic acid (MMA) can be utilized as a biomarker for type 2 diabetes is noteworthy.²⁷ Tryptophan is also known to be altered in type 2 diabetes, and its role in type 1 diabetes needs to be studied in depth.²⁸

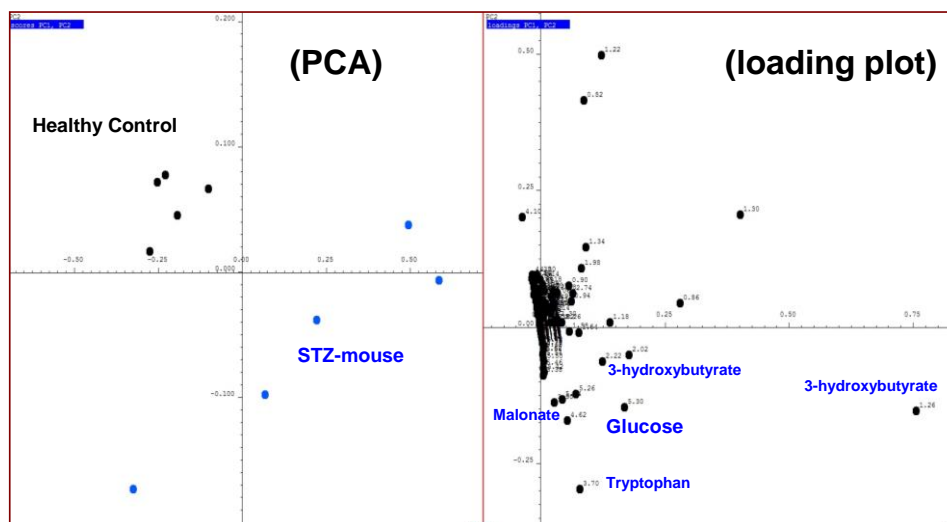


Figure 3. The PCA score plot and the loading plot. The x-axis and y-axis of the PCA plot correspond to the PC1 (38.7%) and the PC2 (16.32%). The loading plot shows the significant contribution of several metabolites for group separation.

Acknowledgements

This work was supported by the Gachon University research fund of 2019 (GCU-2019-0707). This research was also supported by the National Research Foundation of Korea (NRF) funded by the Ministry of Education, Science, and Technology (2018R1D1A1B07050426).

References

1. J. Rui, S. Deng, A. L. Perdigoto, G. Ponath, R. Kursawe, N. Lawlor, T. Sumida, M. Levine-Ritterman, M. L. Stitzel and D. Pitt, *Nat. Commun.* **12**, 5074 (2021)
2. L. Wigger, M. Barovic, A.-D. Brunner, F. Marzetta, E. Schöniger, F. Mehl, N. Kipke, D. Friedland, F. Burdet and C. Kessler, *Nat. Metab.* **3**, 1017 (2021)
3. L. Ikelle, M. I. Naash and M. R. Al-Ubaidi, *Adv. Exp. Med. Biol.* **1185**, 335 (2019)
4. N. C. Holoman, J. J. Aiello, T. D. Trobenter, M. J. Tarchick, M. R. Kozłowski, E. R. Makowski, C. Darryl, C. Singh, J. E. Sears and I. S. Samuels, *J. Neurosci.* **41**, 3275 (2021)
5. J. H. Lee, M. Samsuzzaman, M. G. Park, S. J. Park and S. Y. Kim, *Int. J. Biol. Macromol.* **187**, 409 (2021)
6. J. Danielsson, P. Kangastupa, T. Laatikainen, M. Aalto and O. Niemelä, *World J. Gastroenterol.* **20**, 11743 (2014)
7. J. Blahova, M. Martiniakova, M. Babikova, V. Kovacova, V. Mondockova and R. Omelka, *Pharmaceuticals (Basel)* **14**, 806 (2021)
8. K. V. Gantenbein and C. Kanaka-Gantenbein, *Nutrients* **13**, 1951 (2021)
9. Y. Liu, H. Zhang, S. Wang, Y. Guo, X. Fang, B. Zheng, W. Gao, H. Yu, Z. Chen, R. J. Roman and F. Fan, *Am. J. Physiol. Heart Circ. Physiol.* **320**, H549 (2021)
10. H. C. Park, Y. K. Lee, A. Cho, C. H. Han, J. W. Noh, Y. J. Shin, S. H. Bae and H. Kim, *PLoS One* **14**, e0220506 (2019)
11. J.-S. Hyun, J. Yang, H.-H. Kim, Y.-B. Lee and S. J. Park, *J. Kor. Magn. Reson. Soc.* **22**, 149 (2018)
12. K. Sánchez-Alegría, C. E. Bastián-Eugenio, L. Vaca and C. Arias, *FASEB J.* **35**, e21712 (2021)
13. X Pan, Y Zhu, X Wu, L Liu, R Ying, L Wang, N Du, J Zhang, J Jin, X Meng, F Dai and Y Huang, *Eur. J. Pharmacol.* **893**, 173816 (2021)
14. K. Abramov-Harpaz, M. Pollock-Gagolashvili and Y. Miller, *ACS Chem. Neurosci.* **12**, 3266 (2021)
15. S. J. Park and J. W. Choi, *Arch. Pharm. Res.* **43**, 1017 (2020)
16. C. A. Daykin, P. J. Foxall, S. C. Connor, J. C. Lindon and J. K. Nicholson, *Anal. Biochem.* **304**, 220 (2002)
17. A. Guleria, A. Pratap, D. Dubey, A. Rawat, S. Chaurasia, E. Suresh, S. Phatak, S. Ajmani, U. Kumar and C. L. Khetrpal, *Sci. Rep.* **6**, 35309 (2016)
18. M. Bylesjö, M. Rantalainen, O. Cloarec, J. K. Nicholson, E. Holmes and J. Trygg, *J. Chemom.* **20**, 341 (2006)
19. A. Craig, O. Cloarec, E. Holmes, J. K. Nicholson and J. C. Lindon, *Anal. Chem.* **78**, 2262 (2006)
20. F. Dieterle, A. Ross, G. Schlotterbeck and H. Senn, *Anal. Chem.* **78**, 4281 (2006)
21. J. Trygg, E. Holmes and T. Lundstedt, *J. Proteome Res.* **6**, 469 (2007)
22. S. Wiklund, E. Johansson, L. Sjöström, E. J. Mellerowicz, U. Edlund, J. P. Shockcor, J. Gottfries, T. Moritz and J. Trygg, *Anal. Chem.* **80**, 115 (2008)
23. F. Pesarin, *Multivariate permutation tests: with applications in biostatistics*: Wiley Chichester; 2001
24. B. Worley, S. Halouska and R. Powers, *Analytical biochemistry* **433**, 102 (2013)
25. J. D. Spurrier, *J. Nonparametric Stat.* **15**, 685 (2003)
26. S. Hur, H. Lee, A. Shin and S. J. Park, *J. Kor. Mag. Reson. Soc.* **18**, 10 (2014)
27. M. S. Bjune, C. Lindquist, M. H. Stafsnes, B. Bjørndal, P. Bruheim, T. A. Aloysius, O. Nygård, J. Skorve, L. Madsen and S. N. Dankel, *Biochim. Biophys. Acta Mol. Cell. Biol. Lipids* **1866**, 158887 (2021)
28. F. Zhang, R. Guo, W. Cui, L. Wang, J. Xiao, J. Shang and Z. Zhao, *Ren. Fail.* **43**, 980 (2021)